Molecular Therapy
Original Article

CD39 Produced from Human GMSCs Regulates the Balance of Osteoclasts and Osteoblasts through the Wnt/β-Catenin Pathway in Osteoporosis

Wenbin Wu,[1,5,6] Zexiu Xiao,[1,6] Ye Chen,[1,2,6] Yanan Deng,[1] Donglan Zeng,[1] Yan Liu,[1] Feng Huang,[1] Julie Wang,[2] Yanying Liu,[3] Joseph A. Bellanti,[4] Limin Rong,[5] and Song Guo Zheng[2]

[1]Department of Clinical Immunology Center, The Third Affiliated Hospital of Sun Yat-sen University, Guangzhou 510630, China; [2]Department of Internal Medicine, The Ohio State University College of Medicine and Wexner Medical Center, Columbus, OH 43210, USA; [3]Department of Rheumatology & Immunology, Peking University People's Hospital, Beijing 100044, China; [4]Departments of Pediatrics and Microbiology-Immunology and the International Center for Interdisciplinary Studies of Immunology (ICISI), Georgetown University Medical Center, Washington, DC 20057, USA; [5]Department of Spine Surgery, The Third Affiliated Hospital of Sun Yat-sen University, Guangzhou 510630, China

Osteoporosis is a disease in which the density and quality of bone are reduced, causing bones to become weak and so brittle that a fall or even mild stresses can cause a fracture. Current drug treatment consists mainly of antiresorptive agents that are unable to stimulate new bone formation. Our recent studies have defined a critical role of gingiva-derived mesenchymal stem cells (GMSCs) in attenuating autoimmune arthritis through inhibition of osteoclast formation and activities, but it remains to be ruled out whether the administration of GMSCs to patients with osteoporosis could also regulate osteoblasts and eventually affect bone formation and protection. With the use of an ovariectomized mouse model, we here demonstrated that adoptive transfer of GMSCs regulated the balance of osteoclasts and osteoblasts, eventually contributing to dynamic bone formation. Validation by RNA sequencing (RNA-seq), single-cell sequencing, revealed a unique population of CD39$^+$ GMSC that plays an important role in promoting bone formation. We further demonstrated that CD39 produced from GMSC exerted its osteogenic capacity through the Wnt/β-catenin pathway. Our results not only establish a previously unidentified role and mechanism of GMSC for bone promotion but also a potential therapeutic target for management of patients with osteoporosis and other bone loss conditions.

INTRODUCTION

Osteoporosis-induced fractures are becoming more commonly seen in women over the age of 55 and in men after the age of 65, leading to severe bone-related diseases and increased mortality and health care costs.[1] Although the long-term use of bisphosphonates can reduce the risk of fracture in patients with osteoporosis, their therapeutic effect is slow, requiring long-term treatment cycles and an accompanying increased risk of adverse events.[2,3] Consequently, there is an urgent need for development of new therapeutic agents for regulating bone resorption and formation in patients with osteoporosis.

Mesenchymal stem cells (MSCs) are stromal cell progenitors with significant differentiation and immunomodulatory effects that hold potential promise for combating osteoporosis.[4–6] Gingival tissue-derived MSCs (GMSCs) are a homogeneous population of MSCs isolated from human gingiva that proliferate more rapidly than bone marrow-derived MSCs (BMSCs).[7–11] More importantly, recent studies have suggested that GMSCs may have a superior role in treating xenograft-versus-host diseases than BMSCs.[12]

Previous studies have shown that GMSCs can inhibit T helper (Th)1, Th17 function; upregulate regulatory T cell (Treg) induction; promote macrophage polarization to M2; and inhibit inflammatory cell infiltration at the injury site in a variety of different rheumatic and allergic diseases.[12–17] Recent studies have also shown that GMSCs can directly regulate osteoclast activity and inhibit bone erosion in autoimmune arthritis.[18] Based upon these observations, it would be of interest to investigate whether GMSCs can treat osteoporosis by promoting osteoblastogenesis and subsequent bone formation.

Here, we evaluated the therapeutic potential of GMSCs in treating osteoporosis induced by estrogen deficiency in an ovariectomy (OVX)-induced osteopenic model. After 8 weeks of treatment, GMSCs were shown to have a clear therapeutic effect on trabecular bone densities. GMSC infusion significantly decreased frequency of osteoclasts and increased osteogenic index *in vivo*. To identify underlying molecular mechanism(s), we demonstrated that GMSCs

Received 18 October 2019; accepted 3 April 2020;
https://doi.org/10.1016/j.ymthe.2020.04.003.

[6]These authors contributed equally to this work.

Correspondence: Song Guo Zheng, MD, PhD, Department of Internal Medicine, The Ohio State University College of Medicine and Wexner Medical Center, Columbus, OH 43210, USA.
E-mail: songguo.zheng@osumc.edu
Correspondence: Limin Rong, MD, PhD, Department of Spine Surgery, The Third Affiliated Hospital of Sun Yat-sen University, Guangzhou 510630, China.
E-mail: ronglm@mail.sysu.edu.cn

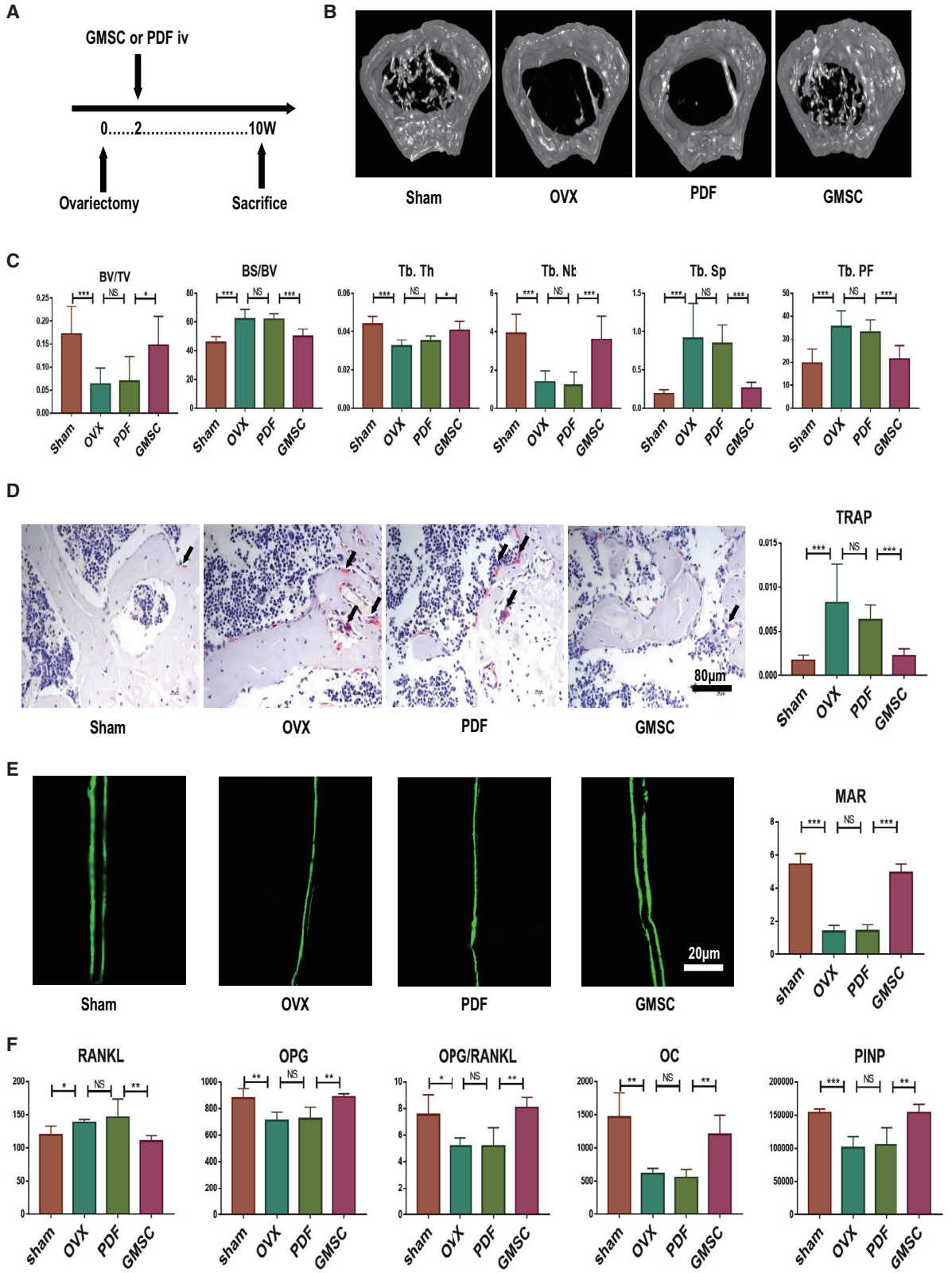

(legend on next page)

can migrate and stay in the bone marrow and other organs after infusion. We also identified that CD39 inhibitor (POM-1) markedly increased the osteogenic potential of GMSCs *in vitro* and almost completely abolished the therapeutic effect of GMSCs on osteoporosis. At the molecular level, we further observed that CD39 produced from GMSCs promoted bone formation through the Wnt/β-catenin pathway. Collectively, our results suggest that the properties of GMSCs not only highlight the key role of the CD39 signal pathway in regulating the balance between osteoclasts and osteoblasts in GMSC function but also may offer potential therapeutic promise for patients with osteoporosis and other bone-loss conditions.

RESULTS

Infusion of GMSCs Alleviates Osteoporosis in OVX Mice

Our recently published study showed that infusion of GMSCs can regulate osteoclasts and inhibit bone erosion in autoimmune arthritis;[18] as such, we sought to determine whether GMSCs can treat osteoporosis by promoting osteoblastogenesis and promoting bone formation. We evaluated the therapeutic potential of GMSCs in osteoporosis induced by estrogen deficiency, which is the most common cause of osteoporosis worldwide, using the OVX-induced osteopenia model.[19]

Each osteoporosis mouse received an intravenous injection of 2 million GMSCs or control cells, 14 days after OVX, following which, all treated mice were sacrificed at 56 days after cell injection (Figure 1A). Since bone loss consistently occurred at 14 days after OVX,[20] the rationale of infusion of GMSCs at this time point attempted to have significant therapeutic value. As expected, the distal femoral trabecular bone was sparse and discontinuous in the OVX group, and GMSC infusion showed a clear therapeutic effect on osteoporosis compared to the control cell prepuce-derived fibroblast (PDF) treatment (Figure 1B). In addition, we observed that bone volume/tissue volume (BV/TV), trabecular thickness (Tb.Th), and trabecular number (Tb.Nb) were all greater in GMSC-treated than in the control cell-treated or OVX model-only groups (Figure 1C). In addition, bone surface area/bone volume (BS/BV), trabecular spacing (Tb.Sp), and trabecular pattern factor (Tb.PF) were also significantly lower in GMSC-treated OVX compared to the OVX model and PDF-treated OVX (Figure 1C). These results demonstrate that GMSC treatment significantly alleviates the osteoporosis in OVX mice.

GMSC Infusion Diminishes Osteoclast Formation and Promotes Bone Formation *In Vivo*

To determine further why GMSCs alleviate the osteoporosis, we analyzed osteoblasts and osteoclasts in bones of OVX mice through tartrate-resistant acid phosphatase (TRAP) staining assessment and dynamic bone formation. With respect to osteoclasts status, we not only observed that GMSC treatment resulted in a lower number of $TRAP^+$ osteoclasts *in vivo* compared to untreated controls but also that the PDF treatment group (Figure 1D) and histomorphometric analysis of osteoclasts' surface ratio decreased significantly (Figure 1D). With the use of calcein to show osteoid mineralization function, we found a higher mineral apposition rate (MAR) in the GMSC group (Figure 1E). Consistent with this finding, the clinical bone formation markers osteocalcin (OC) and procollagen type 1-N-terminal propeptide (PINP) increased in serum after GMSC treatment (Figure 1F). We also analyzed the osteoprotegerin (OPG)-receptor activator of nuclear factor κB (NF-κB) ligand (RANKL) system, since this axis is a crucial determinant of bone remodeling.[21] The circulating RANKL increased after OVX and reduced in GMSC-treated mice relative to control mice, whereas OPG showed the opposite changes. In addition, the OPG/RANKL ratio showed more obvious results (Figure 1F). Taken together, GMSC treatment alleviates the osteoporosis by diminishing osteoclast formation and promoting osteoblast formation.

GMSCs Contribute to Bone Formation after Injection into Mice

To determine whether GMSCs contributed to bone formation solely by themselves without the participation of the immunoregulatory function *in vivo*, we used a cell transplantation model (Figure 2A). We observed that GMSC administration in immunocompromised mice formed tissue clumps and generated bone organoids detected by micro-computed tomography (micro-CT) (Figure 2B). To track the distribution of GMSCs in the ovariectomized mouse model, we used an in vivo imaging systems (IVIS) imaging system (Figure 2C). GMSCs not only migrated into lung and liver but also into upper and lower limbs (Figure S1A). Interestingly, the distribution of GMSCs could not only be clearly visualized in bone marrow tissue (Figure 2D) but also detected by labeled GMSCs by flow cytometry (Figure S1B) and fluorescence microscopy (Figure S1C). We systemically tracked the distribution of GMSCs in bone marrow and found GMSCs engrafted to the host tissue for more than 8 weeks (Figure 2E). Thus, GMSCs can migrate into bone marrow to achieve long-term therapeutic effects, presumably through paracrine and immune-regulatory functions that modulate the local milieu. In addition to their robust

Figure 1. Infusion of GMSCs Alleviates Osteoporosis by Diminishing Osteoclast Formation and Promoting Bone Formation in OVX Mice

OVX mice were treated with gingiva-derived mesenchymal stem cells (GMSCs) or control cells prepuce-derived fibroblasts (PDFs) or PBS (OVX) on 14 days after surgery, and mice were sacrificed on 56 days after injection. (A) Study design of the experiment. Femur, tibiae, and blood were sampled at sacrifice. (B) Representative micro-CT images illustrating trabecular bone mass of the distal metaphysis of femur. Region of interest (ROI) was defined 1–2 mm away from epiphyses; n = 8. (C) Corresponding parameters showing the treatment of osteoporosis by GMSC therapy. BV/TV, bone volume/tissue volume; BS/BV, bone surface area/bone volume; Tb.Th, trabecular thickness; Tb.Nb, trabecular number; Tb.Sp, trabecular spacing; Tb.PF, trabecular pattern factor; n = 8. (D) Representative TRAP-stained femur tissue sections from the different groups' mice. The ratio of TRAP-positive cells in the field was counted in each group; n = 8. (E) Representative calcein-labeling images exhibiting bone formation rates. Mice received double injection of 10 mg/kg calcein at 14 and 2 days before sacrifice. Corresponding parameters showing osteoid mineralization function. MAR, mineral apposition rate; n = 4. (F) The levels of bone-remodeling markers secretion from the sham, model, PDF, and GMSC treatment groups of OVX mice; n = 5. The results represent three independent experiments (mean ± SEM), *p < 0.05, **p < 0.01, ***p < 0.001 by Mann-Whitney tests or t test or ANOVA test.

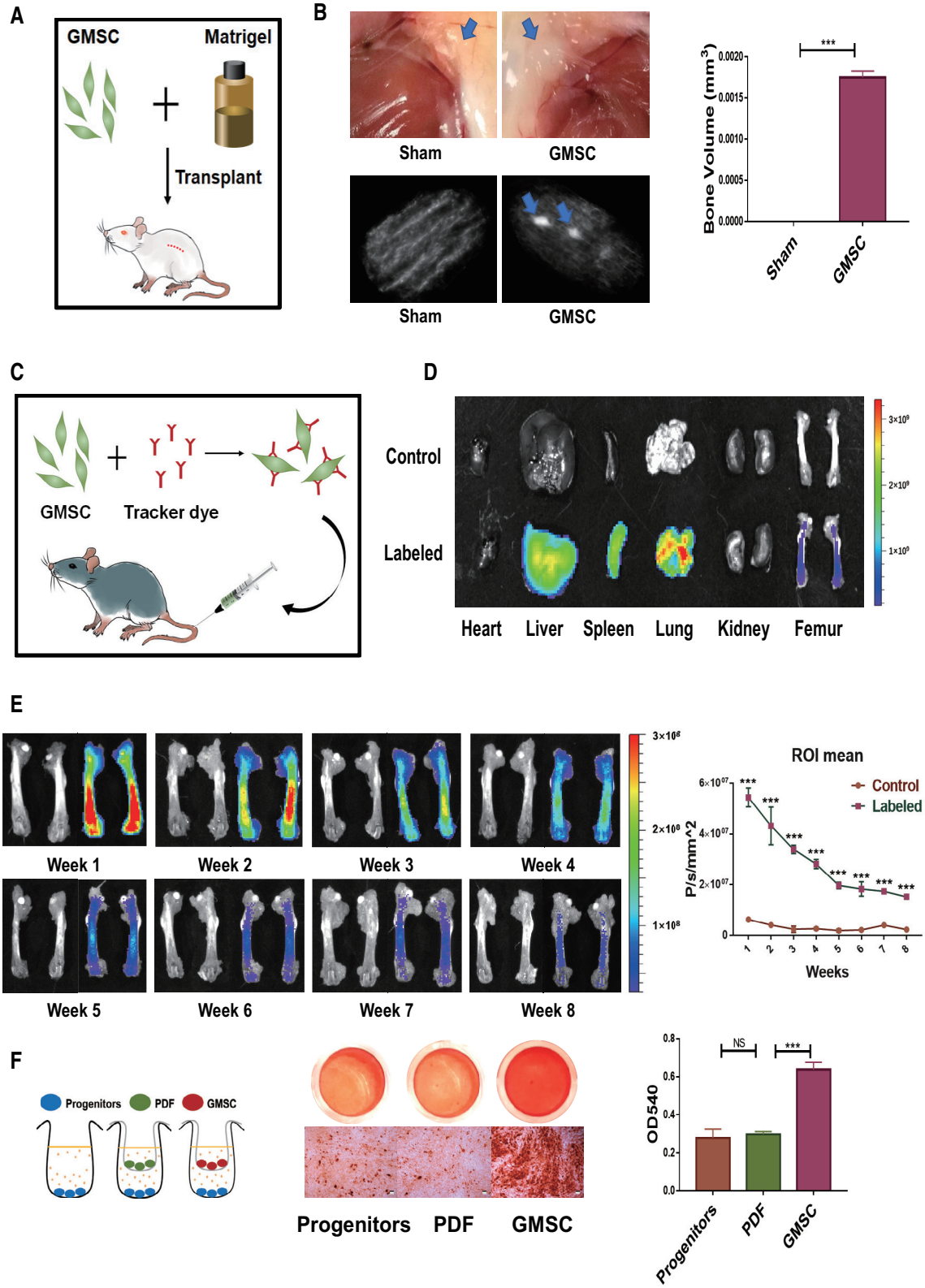

(legend on next page)

osteogenesis capacity, we found that GMSCs promoted osteoblast progenitor mineralization (Figure 2F). Based upon our previous study indicating that GMSCs maintain their phenotype, osteogenic capacity, and functional activity following injection into C57BL/6 mice,[22] we also found that GMSCs can differentiate into osteoblasts in mouse bone marrow tissue (Figure S1D). Our current findings strongly suggest that GMSCs can directly contribute to bone formation *in vivo*.

Osteogenic Function of GMSCs Depends upon CD39

To identify the molecular signaling pathway(s) associated with GMSC function, we used an RNA sequencing (RNA-seq) methodology to analyze the differences between GMSCs and PDFs. We found that RNA-seq could identify a much higher transcriptional level of CD39 in GMSCs than in control cells, a difference that achieved significant statistical significance (Figure 3A). This observation was also further validated by the demonstration that the expression of CD39 was significantly greater in GMSCs than in fibroblast via qPCR and western blot analyses (Figures 3B and 3C). We observed that pretreatment of GMSCs with a CD39 inhibitor (POM-1), but not other inhibitors, almost completely abolished their osteogenic activity *in vitro* (Figure 3D). These results were also confirmed by quantification of hexadecyl pyridinium chloride monohydrate (Figure 3D). Pretreatment of POM-1 at doses employed failed to change GMSC viability, including apoptotic and cell-proliferative activity and excluding the possibility that these inhibitors nonspecifically affected GMSCs and then altered their functional activity, supporting our previous findings (Figures S2A–S2C). Based on single-cell sequence properties, we identified five GMSC clusters used by t-distributed stochastic neighboring clusters that significantly displayed higher activity than that in other clusters (Figure 3E). Interestingly, BMP-2 and Runx2, genes that clearly associated with osteogenesis, were also found to be higher in cluster 4 activity than in other clusters (Figure 3E). Based upon these observations, it seems likely that CD39 might reflect the osteogenesis function of GMSCs. With the use of qPCR and western blotting, we further examined the expression of genes related to osteoblast formation and development, including Runx2 and Osx. Blockade of CD39 on GMSCs significantly suppressed the expression of these genes as well (Figures 3F and 3G).

Antagonist of CD39 Impairs the Bone Remodeling of GMSCs in Osteoporosis

We further explored whether these mechanisms could have effects of GMSCs on bone remodeling during osteoporosis *in vivo*. We chose the CD39-specific inhibitor to pretreat GMSCs and then transferred these GMSCs or unpretreated GMSCs into OVX mice (Figure 4A). As shown in Figure 4, GMSCs displayed a clear therapeutic effect on bone density, increased bone volume and trabecular parameters, decreased the frequency of $TRAP^+$ osteoclasts, promoted bone formation, and regulated the biomarkers in bone remodeling. Blockade of CD39 signal on GMSCs almost completely abrogated their effects on these manifestations (Figures 4B–4F). We additionally used short hairpin (sh)RNA to knock down CD39 in GMSCs to confirm the function *in vivo* experiments (Figures 4G and 4H; Figure S3).

CD39 Contributes to the Immunomodulation of GMSCs in Osteoporosis

In addition to osteoblasts and osteoclasts, immune cells and inflammatory cytokines play an important role in the development of osteoporosis as well.[23] A number of studies have shown that Tregs can inhibit osteoporosis in OVX mice.[24–26] Moreover, previous research found that interleukin (IL)-17, produced by Th17 cells, further increases RANKL expression and promotes osteoclast differentiation.[27] Many cytokines contribute to Th17 differentiation,[28–30] which may also directly or indirectly promote osteoclast. We previously reported that GMSCs not only suppressed Th1 and Th17 but also promoted Treg induction in mouse and humanized animal model systems.[12,13] To identify the immunoregulatory function of GMSCs in osteoporosis, we measured the levels of lymphocytes, cytokines, and osteoclast precursors in different groups.

Regulatory T cells were significantly increased, and the inflammatory cells (interferon [IFN]-γ^+, IL-17^+) were decreased in bone marrow cells of GMSC-treated OVX compared to the OVX model and PDF-treated OVX (Figures 5A and 5B). Pretreatment of GMSCs with POM-1 also significantly abolished these changes (Figures 5A and 5B). We also observed that osteoclast precursors ($CD115^+$ $CD11b^+$) were reduced in bone marrow cells after GMSC treatment (Figure 5C). To confirm this finding, we isolated $CD11b^+$ cells from bone marrow to induce osteoclast formation and found that the osteoclast-inducing capacity of monocytes in the GMSC-treated group was markedly lower than in other groups (Figure 5D). These results further highlight the contribution of CD39 in promoting the immunomodulatory function(s) of GMSCs in bone remodeling and in alleviating the progress of osteoporosis.

Figure 2. GMSCs Contribute to Bone Formation after Injection into Mice

(A and B) A 50-μL Matrigel plug containing 1×10^5 GMSCs was implanted subcutaneously in immunocompromised mice. (A) Schematic of the transplantation model. (B) Representative gross look of subcutaneous tissue and micro-CT images illustrating organoids in a transplantation model. The quantification of bone volumes in subcutaneous tissues, n = 3. (C–E) 2×10^6 of GMSCs were fluorescently labeled with DiR and adoptively infused into C57BL/6 mice. (C) Schematic of the GMSC tracking model. (D) Representative digital IVIS images in different groups on 3 days after injection, n = 3. (E) Representative digital IVIS images and quantification of fluorescence intensity in different time points, n = 3. (F) GMSCs and osteoblast precursors (OBPs) cocultured (GMSCs to OBPs = 1:10) in the Transwell system; then induced osteogenesis followed with alizarin red staining. Representative gross look and image under microscope were shown under different conditions and the quantification by hexadecyl pyridinium chloride monohydrate in different treatment groups n = 3. The results represent three independent experiments (mean ± SEM), *$p < 0.05$, **$p < 0.01$, ***$p < 0.001$ by Mann-Whitney tests or t test or ANOVA test.

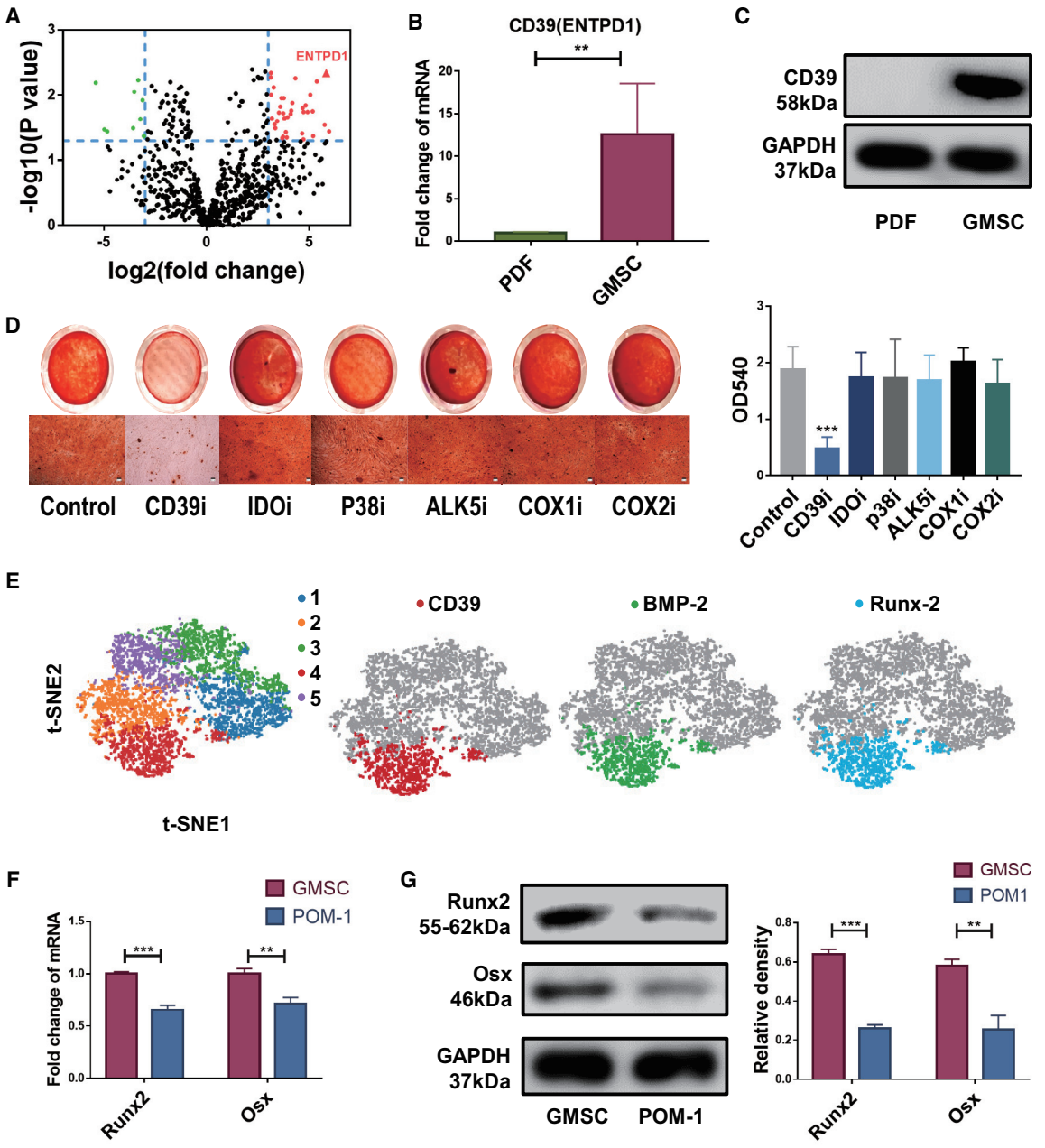

Figure 3. Osteogenic Function of GMSCs Depends on CD39

Gingiva-derived mesenchymal stem cells (GMSCs) and prepuce-derived fibroblasts (PDFs) derived from three different individuals. Fresh cells or resuscitated stored cells from the third to the fifth passages were used in the experiments. (A) RNA sequence volcano map for GMSCs and control cell PDFs. (B) qPCR result showing the CD39 expression levels of the GMSCs and PDFs, n = 3. (C) Western blotting of the CD39 levels of the GMSCs and PDFs, n = 3. (D) GMSCs were pretreated with CD39 inhibitor (POM-1, 100 μM), IDO inhibitor (1-MT, 500 μM), p38 inhibitor (SB203580, 10 μM), ALK5 inhibitor (10 μg/mL), selective cyclooxygenase 1 (COX-1) inhibitor (indomethacine, 20 μM), and selective COX-2 inhibitor (NS-398, 20 μM) overnight; then induced osteogenesis followed with alizarin red staining. Representative gross look and image under microscope were shown under different conditions and the quantification by hexadecyl pyridinium chloride monohydrate in different treatment groups, n = 3. (E) Five GMSC clusters, t-distributed stochastic neighbor embedding (t-SNE) of GMSCs, colored by clustering. CD39, BMP-2, and Runx2 expression in single-cell sequence clusters. (F) qPCR result showing genes related to osteoblast formation and development expression on GMSCs and POM-1-pretreated GMSCs, n = 3. (G) Runx2 and Osx expression on GMSCs and POM-1-pretreated GMSCs was determined using western blotting. The relative density to GAPDH was shown, n = 3. The results represent three independent experiments (mean ± SEM), *p < 0.05, **p < 0.01, ***p < 0.001 by Mann-Whitney tests or t test or ANOVA test.

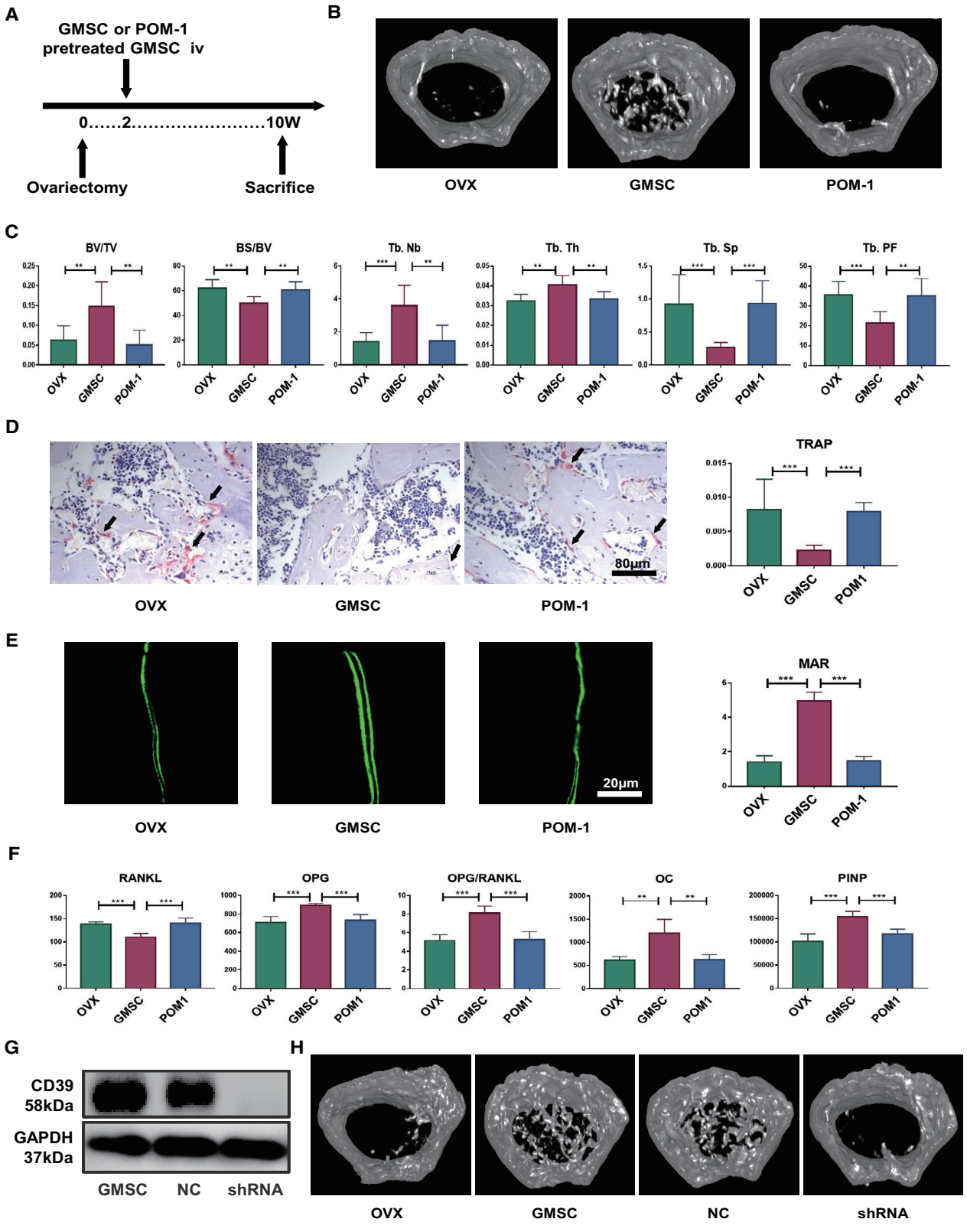

(legend on next page)

GMSCs Exert Their Osteogenic Capacity by CD39 through the Wnt/β-Catenin Pathway

In order to explore underlying mechanism(s) of CD39 on GMSCs in regulating osteogenic functions, we used a quantitative RT-PCR array to compare GMSCs and POM-1-pretreated GMSCs. We found that Wnt3A displayed a remarkably high transcript level in GMSCs compared to blockade of the CD39 population (Figure 6A). The protein level of Wnt3A also decreased in POM-1-pretreated GMSCs (Figure 6B). In addition, data obtained from laser confocal experiments indicated that overnight pretreatment of GMSCs with the CD39 inhibitor decreased the concentration of β-catenin in the nucleus of GMSCs (Figure 6C). We further demonstrated that the osteogenic function of POM-1-pretreated GMSCs was restored by addition of Wnt3A protein to the osteogenic medium (Figure 6D). These results suggest that the CD39-specific inhibitor suppresses the expression of the Wnt3A gene, thereby reducing intranuclear transcription of β-catenin and ultimately resulting in a loss of the osteogenic potential of GMSCs. Since Wnt signaling pathway is one of the strongest paracrine signals stimulating osteogenesis, we further demonstrated that blocking CD39 on GMSCs affected their capacity to secrete soluble (s)Wnt3A in the cell culture supernatant (Figure 6E). These results also confirmed that blocking CD39 reduced the paracrine mineralization-inducing effects of osteoblast progenitor cells (Figure 6F).

DISCUSSION

There are over 200 million individuals suffering from osteoporosis throughout the world and more than one-third of menopausal women who experience osteoporotic fractures after the age of 50.[31] Current drug treatment regimens consist mainly of antiresorptive agents, which are unable to stimulate new bone formation. The only osteoanabolic-approved drug, recombinant parathyroid hormone (rPTH [teriparatide]), must be discontinued after 2-year usage because prolonged duration of treatment may increase risk of bone neoplasia, limiting its usefulness for life-long treatment.[2]

GMSCs, like other MSCs, are progenitor cells with a capacity of immunomodulation and repair regeneration.[7] We have previously reported that GMSC infusion may be a promising therapeutic approach for rheumatoid arthritis, graft-versus-host disease (GVHD), type 1 diabetes mellitus (T1DM), stroke, and other autoimmune and/or inflammatory diseases.[12–16] We recently reported GMSCs suppressed osteoclastogenesis and bone erosion in autoimmune arthritis.[18] In the current study, we demonstrated that GMSCs not only directly suppressed the formation of osteoclasts but also promoted osteoblast formation, eventually contributing to the balance of the osteoblast-to-osteoclast ratio and to potential treatment of osteoporosis. This leads to an important implication: that GMSCs, in the near future, may be deployed in clinical transplantation therapy. Indeed, our recent preclinical safety studies have demonstrated that GMSC infusion therapy is both feasible and fairly safe,[22] moving this possibility forward toward eventual clinical implementation.

Due to the low immunogenicity of MSCs, GMSCs have been demonstrated to be useful mouse and humanized animal models.[12,13] In the present study, we chose fibroblasts as a control cell, not only because of their morphologic similarity to GMSCs, but also because of their diverse biological activities. This control has helped to exclude the possibility of a nonspecific role that GMSCs may be playing in the treatment of osteoporosis.

We recently systemically studied the dynamic distribution and fates of GMSCs through various routes of injection and found that GMSCs are distributed and survive in many important organs.[22] It has been previously reported that although a part of MSCs are trapped in the lungs after injection into mice, enough cells are still available to reach their bone marrow target to ensure stable engraftment.[32] Here, we confirmed that transferred GMSCs can distribute in bone marrow. Therefore, it is reasonable to conclude that GMSCs can specifically regulate bone remodeling in their bone marrow niche.

There is now convincing evidence to document that MSCs have osteogenic repair ability.[33,34] In recent years, additional studies have shown that MSCs can also lead to bone mineralization in animal model systems.[35] In addition, MSCs can support microenvironments for bone promotion in host tissue. As previously reported, MSCs may promote osteoblastogenesis by reducing tumor necrosis factor (TNF)-α levels at the injured site. Mechanistically, this occurs by the known action of TNF-α to inhibit osteoblastogenesis by inhibiting the expression of essential transcription factors for bone formation, although the TNF-α receptor signal is somewhat complicated.[36–38] An interesting experimental study showed that transplanted MSCs promote fracture healing by expressing BMP-2, which induces bone and cartilage formation.[39] It was also proved that vascular endothelial growth factors secreted by MSCs enhance osteoblast proliferation and differentiation.[40] Herein, we have shown that GMSCs not only display strong osteogenic differentiation capability but also manifest a facilitated

Figure 4. Antagonist of CD39 Impairs the Bone Remodeling in Osteoporosis

OVX mice were treated with GMSCs or CD39 blocking GMSCs (POM-1) or PBS (OVX) or transfected GMSCs on 14 days after surgery, and mice were sacrificed on 56 days after injection. (A) Study design of the experiment. Femur, tibiae and blood were sampled at sacrifice. (B) Representative micro-CT images illustrating trabecular bone mass of the distal metaphysis of femur. ROI was defined 1–2 mm away from epiphyses, n = 8. (C) Corresponding parameters showing blockade of the CD39 signal on GMSCs almost completely abrogated their effects, n = 8. BV/TV, bone volume/tissue volume; BS/BV, bone surface area/bone volume; Tb.Th, trabecular thickness; Tb.Nb, trabecular number; Tb.Sp, trabecular spacing; Tb.PF, trabecular pattern factor. (D) Representative TRAP-stained and calcein-labeling images in each group. The ratio of TRAP-positive cells in the field and the mineral apposition rate was counted, n = 8. (E) Representative calcein-labeling images in each group. The mineral apposition rate was counted, n = 4. (F) The levels of bone-remodeling markers secretion from the model, GMSCs, and GMSCs pretreated with CD39 inhibitor groups of OVX mice, n = 5. (G) CD39 expression on GMSCs and transfected GMSCs was determined using western blotting, n = 3. (H) Representative micro-CT images illustrating trabecular bone mass of the distal metaphysis of femur, n = 5. The results represent three independent experiments (mean ± SEM), *p < 0.05, **p < 0.01, ***p < 0.001 by Mann-Whitney tests or t test or ANOVA test.

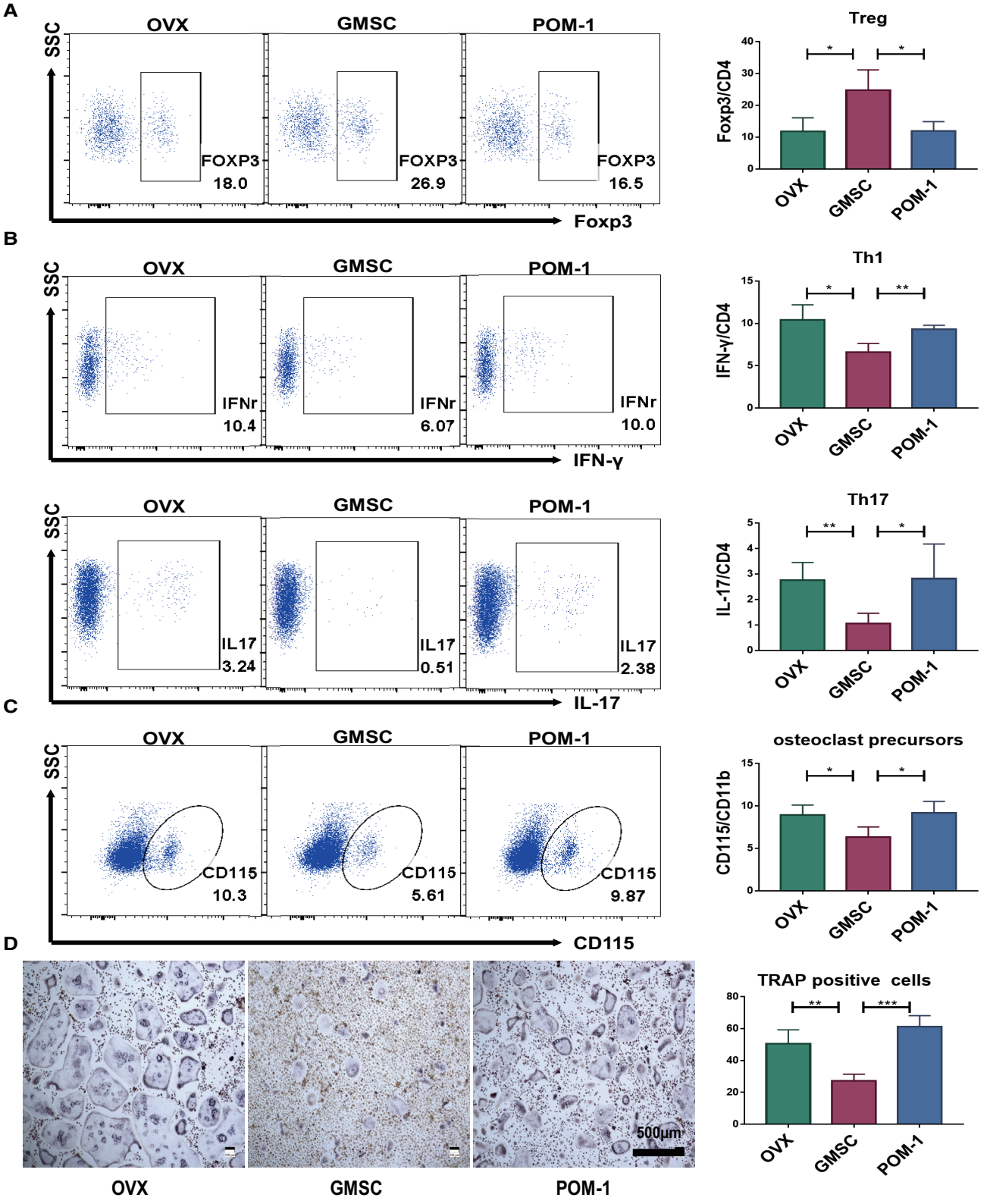

(legend on next page)

in vitro and *in vivo* capacity for osteogenesis from osteoblast progenitors.

CD39 is a transmembrane hydrolase that degrades extracellular ATP to adenosine, which is known to display anti-inflammatory effects on immune cells.[41–43] Moreover, CD39 has been previously reported to be involved in the suppressive activity of $CD4^+$forkhead box p3 $(Foxp3)^+$ Tregs and $CD8^+$ Tregs,[44–47] which are not only known to be important immune suppressors but also to inhibit directly or indirectly osteoclast activity.[48–51] In our previous study, we found the suppressive function of GMSCs to be carried out by the CD39-CD73-adenosine signal pathway, and pretreatment of GMSCs with a CD39 inhibitor distinctly, significantly abolished their immunosuppressive function.[18] Adenosine receptors also regulate bone remodeling. The A1 receptor is constitutively activated and required for osteoclast differentiation and function, whereas the A2A receptor exerts the opposite effect.[52] A2B adenosine receptor has been reported to promote MSC differentiation to osteoblasts and bone formation.[53] Recently, it has been demonstrated that CD39/CD73 expression and extracellular adenosine levels in the bone marrow are substantially decreased in animals with osteoporotic bone loss.[54] Here, we demonstrated that CD39 plays an important role in the osteogenic function of GMSCs, partially through the Wnt/β-catenin axis. Thus, CD39 signaling not only regulates the suppression of osteoclasts and promotion of osteoblasts but also provides a crucial molecular target for treatment of bone-related diseases.

The Wnt proteins are a family of 19 highly conserved, secreted glycoproteins that display important roles in regulating osteoblast lineage cells.[55,56] β-catenin will enter the nucleus when Wnt binds to Frizzled receptors and their coreceptors; subsequently, β-catenin stimulates the transcription of osteogenic target genes, such as Runx2 and Osx.[57,58] In addition, canonical Wnt signaling is known to suppress osteoclastogenesis by inducing OPG, which regulates bone remodeling.[59,60] The Wnt signaling pathway has, therefore, emerged as a critical regulatory component of processes that control bone formation and bone resorption, therefore providing new therapeutic targets for the management of osteoporosis.[61]

In conclusion, we have demonstrated that GMSCs regulate the balance of osteoclasts and osteoblasts in osteoporosis by a CD39-dependent Wnt/β-catenin signaling pathway. Our data suggest that application of GMSCs represents a new, potential therapeutic approach for patients with osteoporosis and other related bone-related diseases and highlight the key role of CD39 in GMSC function.

MATERIALS AND METHODS

Mice

C57BL/6 mice (female, 6–8 weeks old) and nonobese diabetic/severe combined immunodeficient (NOD/SCID) mice (female, 6–8 weeks old) were obtained from Beijing Vital River Laboratory Animal Technology and Jackson Laboratory. All mice were housed in the center of experimental animals of the Sun Yat-sen University and The Ohio State University Wexner Medical Center. The use of animals was approved by the Institutional Animal Care and Use Committee at Sun Yat-sen University and The Ohio State University.

GMSCs

Human gingival tissue samples were collected by routine dental procedures at the Oral and Maxillofacial Surgery Clinic in the Division of Dentistry at the Third Affiliated Hospital of Sun Yat-sen University and The Ohio State University and were approved by the medical ethics committees of the Institutional Review Boards (IRB) at the two institutions. Human GMSCs were prepared from these samples, as previously described.[13,62]

Mouse Models

At 8 weeks of age, mice were either sham or ovariectomized. Surgically removed ovaries were examined by the histology to verify successful ovariectomy. 2×10^6 GMSCs or human dermal fibroblasts (control cells) were intravenously injected into each mouse on day 14 after surgery. To determine underlying mechanisms, GMSCs were pretreated with CD39 inhibitor POM-1 (Tocris Bioscience; 100 μM) overnight and washed twice with PBS before being injected into mice. Mice were subsequently analyzed at 18 weeks of age for assessment of dynamic bone formation by intraperitoneal calcein injection (10 mg/kg per mouse) at 14 days and 2 days prior to completion of the experiments, which were repeated at least three times. GMSCs that had been used at each time period were obtained from different donors, and mice in each experimental time interval received the same cell population from the same donor.

Micro-CT Analysis

CT imaging was performed using Siemens Inveon CT Scanner, and voxel size is 9 μm. Image reconstruction was carried out using Inveon Acquisition workplace software. Trabecular bone densities were manually segmented from cortical bone, and trabecular bone parameters were analyzed over 100 slices, starting 1 mm distal from the growth plate.

Figure 5. CD39 Contributes to the Immunomodulation of GMSCs in Osteoporosis

OVX mice were treated with GMSCs, CD39-blocking GMSC (POM-1), or PBS (OVX) 14 days after surgery, and mice were sacrificed on 56 days after injection. (A) The expression of Foxp3 by $CD4^+$ T cells in bone marrow cells was determined by flow cytometry, n = 4. (B) The expression of IFN-γ and IL-17 by $CD4^+$ T cells in bone marrow cells was determined by flow cytometry, n = 4. (C) The osteoclast precursors ($CD115^+$ $CD11b^+$) in bone marrow cells were determined by flow cytometry, n = 4. (D) Isolate $CD11b^+$ cells from bone marrow to induced osteoclast formation, followed with TRAP staining. Representative images of osteoclast generation in each group and TRAP-positive osteoclast numbers of per area under different conditions were quantified, n = 4. The results represent three independent experiments (mean ± SEM), $^*p < 0.05$, $^{**}p < 0.01$, $^{***}p < 0.001$ by Mann-Whitney tests or t test or ANOVA test.

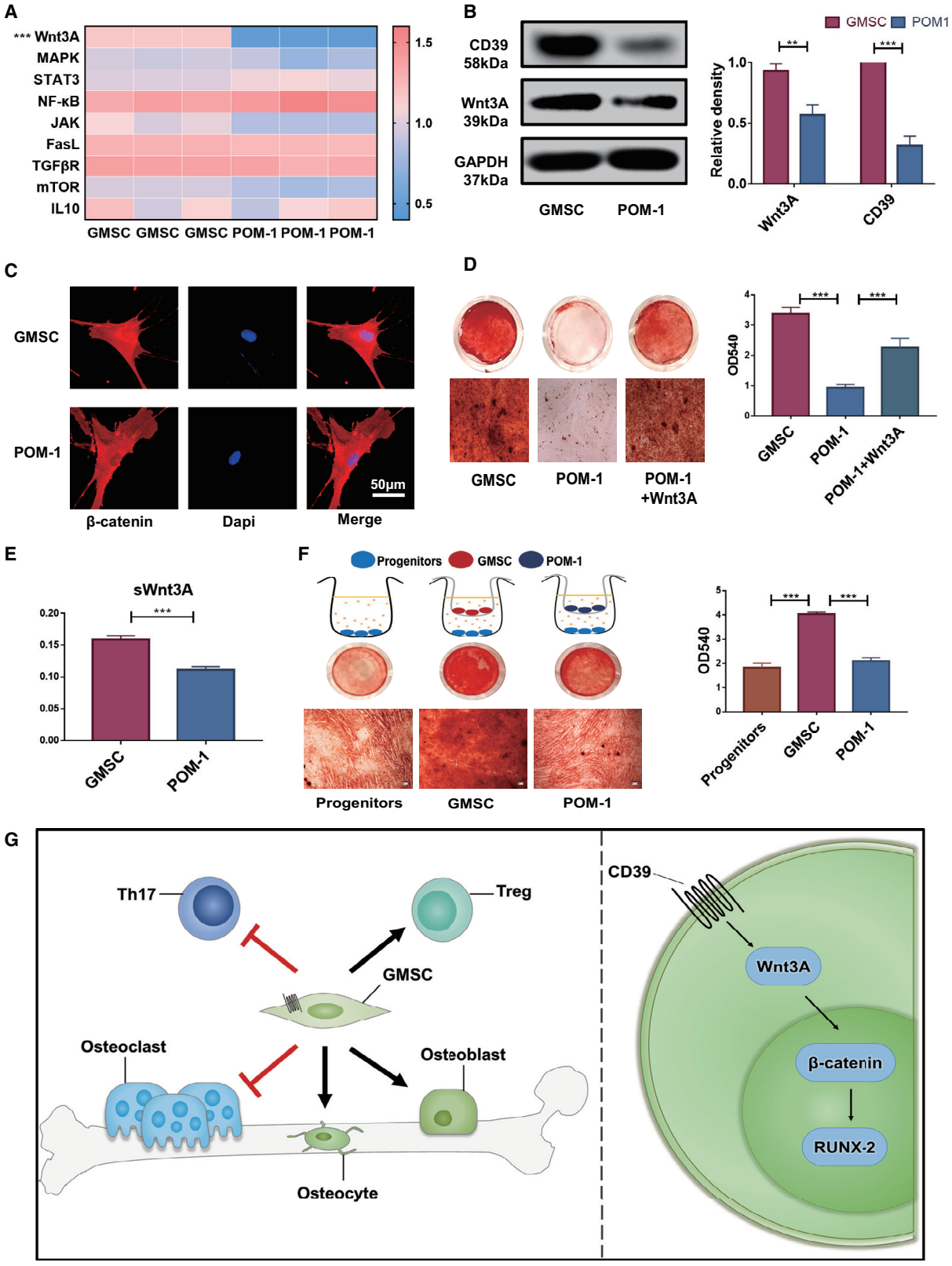

(legend on next page)

ELISA

Mouse OPG, sRANKL, OC, PINP in serum/plasma, and human sWnt3A in cell culture supernatants were measured using the ELISA kit (Elabscience Biotechnology), according to the manufacturer's instruction.

Histology

Mice femurs were fixed in formalin, embedded in paraffin, and sectioned. TRAP staining was performed with a TRAP kit (Sigma-Aldrich; 387A). MAR was performed on methacrylate-embedded, undecalcified plastic sections. All quantifications were performed by digital image analysis.

Flow Cytometric Analysis

For cytometric flow analysis, cells were prepared in single-cell suspensions. Antibodies against mouse CD3, CD4, CD115, IFN-γ, IL-17a, Foxp3, and isotype were obtained from BioLegend. Results were obtained on a Becton Dickinson (BD) fluorescence-activated cell sorting (FACS) Fortessa flow cytometer and analyzed using FlowJo.

Osteoclastogenesis

$CD11b^+$ cells were isolated from bone marrow of mice by autoMACS with biotin anti-mouse CD11b antibody (BioLegend) and anti-biotin MicroBeads (Miltenyi Biotec), purity >95%. The $CD11b^+$ cells were suspended and cultured in 48 wells in α-minimum essential medium (MEM) culture medium (containing 10% fetal bovine serum [FBS]) in the presence of mouse macrophage colony-stimulating factor (M-CSF; 50 ng/mL) for 3 days and then stimulated with mouse RANKL (50 ng/mL) (R&D Systems) and mouse M-CSF (50 ng/mL) (R&D Systems) for an additional 6 days to induce osteoclast formation. To evaluate osteoclast formation, cells were stained with a TRAP kit (Sigma-Aldrich; 387A), according to the manufacturer's instructions, and $TRAP^+$ cells were enumerated by microscopy.[51]

Osteogenesis

BMSCs were purchased from Cyagen Biosciences as osteoblast progenitors (OBPs). OBPs were cocultured with GMSCs (GMSCs to OBPs = 1:10) in a Transwell system using the StemPro Osteogenesis Diff Kit (Gibco), according to the manufacturer's protocol. Calcification was verified by alizarin red staining.

To determine GMSC osteogenesis function, GMSCs were induced using the StemPro Osteogenesis Diff Kit (Gibco), according to the manufacturer's protocol. Calcification was verified by alizarin red staining. Quantification was solubilized by 100 mM hexadecyl pyridinium chloride monohydrate for 30 min and measured at 540 nm. To determine underlying molecular mechanisms in different groups, GMSCs were pretreated with the CD39 inhibitor (POM-1), indoleamine-2,3-dioxygenase (IDO) inhibitor (1-methyl-L-tryptophan [1-MT]; Sigma-Aldrich; 500 μM), p38 inhibitor (SB203580; Sigma-Aldrich; 10 μM), activin receptor-like kinase 5 (ALK5) inhibitor (LY364947; Sigma-Aldrich; 20 μM), selective cyclooxygenase 1 (COX-1) inhibitor (indomethacine; Sigma-Aldrich; 20 μM), or selective COX-2 inhibitor (NS-398; Sigma-Aldrich; 20 μM).

GMSC Transplantation Model

As previously described,[35,63,64], 8- to 10-week-old female immunocompromised mice were anesthetized. A 50-μL Matrigel plug (Corning Matrigel Growth Factor Reduced Basement Membrane Matrix, 356231) containing 1×10^5 GMSCs was implanted subcutaneously, and the contralateral site was injected with a Matrigel plug as a control. Animals were euthanized by CO_2 after 5 weeks. After death, subcutaneous tissues at the injection site were fixed with 4% paraformaldehyde (PFA), and bone formation was detected by micro-CT.

GMSC Tracking in Bone Marrow

To investigate whether transferred GMSCs can migrate into bone marrow, 2×10^6 of GMSCs were fluorescently labeled with DiR (Invitrogen) and adoptively infused into C57BL/6 mice. Femurs of GMSC-transferred mice were imaged using an IVIS imaging system to determine the distribution of GMSCs. Because of limited fluorescence wavelength-detection capability, we used the Cell Tracker Red CMTPX dye (Thermo Fisher Scientific)-labeled GMSCs injected into another cohort of mice. With the use of this modification, the bone marrow cells were detected by a Leica fluorescence microscope and BD FACS Fortessa flow cytometer to confirm the ratio of GMSCs.

Transfection

Lentiviral vectors, expressing an shRNA (sequence 5′-CCTTC TGCAAGGCTATCATTT-3′) against CD39, were designed, constructed, amplified, and purified by GenePharma (Shanghai, China), and a negative control recombinant vector, which expressed green fluorescence protein, was also generated. Transfection was applied for knockdown, according to the manufacturer's protocol (GenePharma). After 8 h of transfection, GMSCs were washed and cultured in normal growth medium for 72 h before use.

Figure 6. GMSCs Exert Their Osteogenic Capacity by CD39 through the Wnt/β-Catenin Pathway

Pretreated with the CD39 inhibitor (POM-1, 100 μM) overnight, GMSCs were used in the experiments. (A) Quantitative RT-PCR array of the GMSCs and POM-1-pretreated GMSCs. (B) Western blotting of CD39 and Wnt3A levels of the GMSCs and POM-1-pretreated GMSCs. The relative density to GAPDH was shown, n = 3. (C) β-catenin expression in the nucleus was detected by immunofluorescence on GMSCs and POM-1-pretreated GMSCs, n = 3. (D) To induce osteogenesis, with or without human Wnt3A protein (R&D Systems [R&D]; 25 ng/mL). Representative gross look, followed with alizarin red staining and image under microscope, was shown under different conditions and the quantification by hexadecyl pyridinium chloride monohydrate in different treatment groups, n = 3. (E) The levels of soluble Wnt3A secretion in cell-culture supernatant from GMSCs or POM-1-pretreated GMSCs, n = 3. (F) GMSCs or POM-1-pretreated GMSCs cocultured with osteoblast precursors (OBPs) (GMSCs to OBPs = 1:10) in the Transwell system; then, induced osteogenesis followed with alizarin red staining. (G) Schematic of the working hypothesis. The results represent three independent experiments (mean ± SEM), *$p < 0.05$, **$p < 0.01$, ***$p < 0.001$ by Mann-Whitney tests or t test or ANOVA test.

qPCR

Total RNA was extracted from GMSCs with a RNeasy Mini Kit (Omega; R6834-2), and cDNA was synthesized using RT-Master Mix (Takara). Runx2, Osx, mitogen-activated protein kinase (MAPK), STAT3, NF-κB, JAK, Fas-L, transforming growth factor β receptor (TGF-βR), mammalian target of rapamycin (mTOR), and IL-10 mRNA expression was quantified by using TB Green Premix Ex Taq II (Takara). Analysis of samples was performed in triplicate, and the relative expression of the above molecules was determined by normalizing the expression of each target gene to glyceraldehyde 3-phosphate dehydrogenase (GAPDH) by using the 2-ΔΔCt method.

Western Blot

GMSCs were collected and lysed by lysing buffer (Sigma). Protein extracts were separated by 10% polyacrylamide-SDS gels and electroblotted onto nitrocellulose membranes (GenScript). After blocking with 5% nonfat dry milk/Tris-buffered saline (TBS), the membranes were incubated with antibodies against CD39 (Abcam), Osx (Abcam), Runx2 (Cell Signaling Technology [CST]), and Wnt3A (Cell Signaling Technology), followed by incubation with horseradish peroxidase (HRP)-conjugated secondary antibody (Cell Signaling Technology). The blots were normalized to GAPDH to read out (Cell Signaling Technology).

RNA-Seq and Single-Cell Sequence

GMSCs and fibroblasts were prepared as described above,[62] and total RNA was extracted with the RNeasy mini kit (Invitrogen). cDNA library construction and Illumina sequencing were completed by Beijing Novogene Bioinformatics Technology. Briefly, sequencing libraries were generated using the NEBNext Ultra RNA Library Prep Kit, following the manufacturer's recommendations. The products were sequenced on an Illumina HiSeq platform using a 125-bp/150-bp paired-end mode. Single cells were encapsulated into emulsion droplets using the Chromium Controller (10x Genomics). Single-cell sequence libraries were constructed using the Chromium Single Cell 30 version (v.)2 Reagent Kit, according to the manufacturer's protocol. RNA-seq data used in this study are available at the NCBI Sequence Read Archive (SRA) database under accession number NCBI: PRJNA540091.

Immunofluorescence Staining

The cell slides were fixed in 1% PFA for 15 min at room temperature, followed by permeabilization in 0.5% Triton X-100 for 20 min, blocking overnight in 6% BSA in PBS-T (PBS containing 0.3% Tween) and incubated with primary antibody (CST; 8480) in blocking solution overnight. The slides were then washed twice in PBS-T and incubated with secondary antibodies (AlexaFluor 675 goat anti-rabbit immunoglobulin G [IgG]; 1:100 in 0.03% BSA) for 2 h before final washes in PBS-T and examined in high-resolution confocal images obtained using a Leica confocal microscope equipped with a 100× objective lens (Leica).

Statistical Analysis

For comparison of treatment and control groups, we performed Mann-Whitney tests (where appropriate), unpaired t tests, paired t tests, and one-way or two-way ANOVA (where appropriate) methods. All statistical analyses were performed by GraphPad Prism software. $p < 0.05$ was considered as statistically significant.

SUPPLEMENTAL INFORMATION

Supplemental Information can be found online at https://doi.org/10.1016/j.ymthe.2020.04.003.

AUTHOR CONTRIBUTIONS

S.G.Z., L.R., and W.W. designed the research and wrote the manuscript. W.W., Z.X., and Y.C. performed the experiments. D.Z. and F.H. provided gingival tissues. Y.D., Yan Liu, J.W., and Yanying Liu provided assistance and guidance on experiments. J.A.B. revised and edited the manuscript. All authors read and approved the final version.

CONFLICTS OF INTEREST

The authors declare no competing interests.

ACKNOWLEDGMENTS

W.W., F.H., and L.R. were, in part, supported by a grant from the National Key R&D Program of China (2017YFA0105801). Z.X. was, in part, supported by a grant from the Chinese Natural Science Foundation (81901657). S.G.Z. and J.W. were, in part, supported by NIH R61 (AR AR073409).

REFERENCES

1. Compston, J.E., McClung, M.R., and Leslie, W.D. (2019). Osteoporosis. Lancet *393*, 364–376.
2. Wright, N.C., Looker, A.C., Saag, K.G., Curtis, J.R., Delzell, E.S., Randall, S., and Dawson-Hughes, B. (2014). The recent prevalence of osteoporosis and low bone mass in the United States based on bone mineral density at the femoral neck or lumbar spine. J. Bone Miner. Res. *29*, 2520–2526.
3. Albert, S.G., and Reddy, S. (2017). Clinical Evaluation of Cost Efficacy of Drugs for Treatment of Osteoporosis: A Meta-Analysis. Endocr. Pract. *23*, 841–856.
4. Uccelli, A., Moretta, L., and Pistoia, V. (2008). Mesenchymal stem cells in health and disease. Nat. Rev. Immunol. *8*, 726–736.
5. Papadopoulou, A., Yiangou, M., Athanasiou, E., Zogas, N., Kaloyannidis, P., Batsis, I., Fassas, A., Anagnostopoulos, A., and Yannaki, E. (2012). Mesenchymal stem cells are conditionally therapeutic in preclinical models of rheumatoid arthritis. Ann. Rheum. Dis. *71*, 1733–1740.
6. Su, W., Li, Z., Jia, Y., Zhu, Y., Cai, W., Wan, P., Zhang, Y., Zheng, S.G., and Zhuo, Y. (2017). microRNA-21a-5p/PDCD4 axis regulates mesenchymal stem cell-induced neuroprotection in acute glaucoma. J. Mol. Cell Biol. *9*, 289–301.
7. Zhang, Q., Shi, S., Liu, Y., Uyanne, J., Shi, Y., Shi, S., and Le, A.D. (2009). Mesenchymal stem cells derived from human gingiva are capable of immunomodulatory functions and ameliorate inflammation-related tissue destruction in experimental colitis. J. Immunol. *183*, 7787–7798.
8. Zhang, X., Huang, F., Chen, Y., Qian, X., and Zheng, S.G. (2016). Progress and prospect of mesenchymal stem cell-based therapy in atherosclerosis. Am. J. Transl. Res. *8*, 4017–4024.
9. Huang, F., Liu, Z.M., and Zheng, S.G. (2018). Updates on GMSCs Treatment for Autoimmune Diseases. Curr. Stem Cell Res. Ther. *13*, 345–349.

10. Li, H., Deng, Y., Liang, J., Huang, F., Qiu, W., Zhang, M., Long, Y., Hu, X., Lu, Z., Liu, W., and Zheng, S.G. (2019). Mesenchymal stromal cells attenuate multiple sclerosis *via* IDO-dependent increasing the suppressive proportion of CD5+ IL-10+ B cells. Am. J. Transl. Res. *11*, 5673–5688.

11. Zhao, J., Chen, J., Huang, F., Wang, J., Su, W., Zhou, J., Qi, Q., Cao, F., Sun, B., Liu, Z., et al. (2019). Human gingiva tissue-derived MSC ameliorates immune-mediated bone marrow failure of aplastic anemia *via* suppression of Th1 and Th17 cells and enhancement of CD4+Foxp3+ regulatory T cells differentiation. Am. J. Transl. Res. *11*, 7627–7643.

12. Huang, F., Chen, M., Chen, W., Gu, J., Yuan, J., Xue, Y., Dang, J., Su, W., Wang, J., Zadeh, H.H., et al. (2017). Human Gingiva-Derived Mesenchymal Stem Cells Inhibit Xeno-Graft-versus-Host Disease *via* CD39-CD73-Adenosine and IDO Signals. Front. Immunol. *8*, 68.

13. Chen, M., Su, W., Lin, X., Guo, Z., Wang, J., Zhang, Q., Brand, D., Ryffel, B., Huang, J., Liu, Z., et al. (2013). Adoptive transfer of human gingiva-derived mesenchymal stem cells ameliorates collagen-induced arthritis via suppression of Th1 and Th17 cells and enhancement of regulatory T cell differentiation. Arthritis Rheum. *65*, 1181–1193.

14. Su, W.R., Zhang, Q.Z., Shi, S.H., Nguyen, A.L., and Le, A.D. (2011). Human gingiva-derived mesenchymal stromal cells attenuate contact hypersensitivity via prostaglandin E2-dependent mechanisms. Stem Cells *29*, 1849–1860.

15. Zhang, W., Zhou, L., Dang, J., Zhang, X., Wang, J., Chen, Y., Liang, J., Li, D., Ma, J., Yuan, J., et al. (2017). Human Gingiva-Derived Mesenchymal Stem Cells Ameliorate Streptozoticin-induced T1DM in mice via Suppression of T effector cells and Up-regulating Treg Subsets. Sci. Rep. *7*, 15249.

16. Zhang, X., Huang, F., Li, W., Dang, J.L., Yuan, J., Wang, J., Zeng, D.L., Sun, C.X., Liu, Y.Y., Ao, Q., et al. (2018). Human Gingiva-Derived Mesenchymal Stem Cells Modulate Monocytes/Macrophages and Alleviate Atherosclerosis. Front. Immunol. *9*, 878.

17. Su, W., Wan, Q., Huang, J., Han, L., Chen, X., Chen, G., Olsen, N., Zheng, S.G., and Liang, D. (2015). Culture medium from TNF-α-stimulated mesenchymal stem cells attenuates allergic conjunctivitis through multiple antiallergic mechanisms. J. Allergy Clin. Immunol. *136*, 423–432.e8.

18. Luo, Y., Wu, W., Gu, J., Zhang, X., Dang, J., Wang, J., Zheng, Y., Huang, F., Yuan, J., Xue, Y., et al. (2019). Human gingival tissue-derived MSC suppress osteoclastogenesis and bone erosion via CD39-adenosine signal pathway in autoimmune arthritis. EBioMedicine *43*, 620–631.

19. Krzeszinski, J.Y., Wei, W., Huynh, H., Jin, Z., Wang, X., Chang, T.C., Xie, X.J., He, L., Mangala, L.S., Lopez-Berestein, G., et al. (2014). miR-34a blocks osteoporosis and bone metastasis by inhibiting osteoclastogenesis and Tgif2. Nature *512*, 431–435.

20. Wronski, T.J., Cintrón, M., and Dann, L.M. (1988). Temporal relationship between bone loss and increased bone turnover in ovariectomized rats. Calcif. Tissue Int. *43*, 179–183.

21. Lacey, D.L., Boyle, W.J., Simonet, W.S., Kostenuik, P.J., Dougall, W.C., Sullivan, J.K., San Martin, J., and Dansey, R. (2012). Bench to bedside: elucidation of the OPG-RANK-RANKL pathway and the development of denosumab. Nat. Rev. Drug Discov. *11*, 401–419.

22. Zhao, J., Wang, J., Dang, J., Zhu, W., Chen, Y., Zhang, X., Xie, J., Hu, B., Huang, F., Sun, B., et al. (2019). A preclinical study-systemic evaluation of safety on mesenchymal stem cells derived from human gingiva tissue. Stem Cell Res. Ther. *10*, 165.

23. Weitzmann, M.N., and Ofotokun, I. (2016). Physiological and pathophysiological bone turnover - role of the immune system. Nat. Rev. Endocrinol. *12*, 518–532.

24. Zaiss, M.M., Sarter, K., Hess, A., Engelke, K., Böhm, C., Nimmerjahn, F., Voll, R., Schett, G., and David, J.P. (2010). Increased bone density and resistance to ovariectomy-induced bone loss in FoxP3-transgenic mice based on impaired osteoclast differentiation. Arthritis Rheum. *62*, 2328–2338.

25. Buchwald, Z.S., Yang, C., Nellore, S., Shashkova, E.V., Davis, J.L., Cline, A., Ko, J., Novack, D.V., DiPaolo, R., and Aurora, R. (2015). A Bone Anabolic Effect of RANKL in a Murine Model of Osteoporosis Mediated Through FoxP3+ CD8 T Cells. J. Bone Miner. Res. *30*, 1508–1522.

26. Yu, M., D'Amelio, P., Tyagi, A.M., Vaccaro, C., Li, J.Y., Hsu, E., Buondonno, I., Sassi, F., Adams, J., Weitzmann, M.N., et al. (2018). Regulatory T cells are expanded by Teriparatide treatment in humans and mediate intermittent PTH-induced bone anabolism in mice. EMBO Rep. *19*, 156–171.

27. Zhao, R. (2013). Immune regulation of bone loss by Th17 cells in oestrogen-deficient osteoporosis. Eur. J. Clin. Invest. *43*, 1195–1202.

28. Luo, Y., and Zheng, S.G. (2016). Hall of Fame among Pro-inflammatory Cytokines: Interleukin-6 Gene and Its Transcriptional Regulation Mechanisms. Front. Immunol. *7*, 604.

29. Ivanov, I.I., McKenzie, B.S., Zhou, L., Tadokoro, C.E., Lepelley, A., Lafaille, J.J., Cua, D.J., and Littman, D.R. (2006). The orphan nuclear receptor RORgammat directs the differentiation program of proinflammatory IL-17+ T helper cells. Cell *126*, 1121–1133.

30. Lu, L., Lan, Q., Li, Z., Zhou, X., Gu, J., Li, Q., Wang, J., Chen, M., Liu, Y., Shen, Y., et al. (2014). Critical role of all-trans retinoic acid in stabilizing human natural regulatory T cells under inflammatory conditions. Proc. Natl. Acad. Sci. USA *111*, E3432–E3440.

31. Cosman, F., de Beur, S.J., LeBoff, M.S., Lewiecki, E.M., Tanner, B., Randall, S., and Lindsay, R.; National Osteoporosis Foundation (2014). Clinician's Guide to Prevention and Treatment of Osteoporosis. Osteoporos. Int. *25*, 2359–2381.

32. Lee, R.H., Pulin, A.A., Seo, M.J., Kota, D.J., Ylostalo, J., Larson, B.L., Semprun-Prieto, L., Delafontaine, P., and Prockop, D.J. (2009). Intravenous hMSCs improve myocardial infarction in mice because cells embolized in lung are activated to secrete the anti-inflammatory protein TSG-6. Cell Stem Cell *5*, 54–63.

33. Chiu, L.H., Lai, W.F., Chang, S.F., Wong, C.C., Fan, C.Y., Fang, C.L., and Tsai, Y.H. (2014). The effect of type II collagen on MSC osteogenic differentiation and bone defect repair. Biomaterials *35*, 2680–2691.

34. Guan, M., Yao, W., Liu, R., Lam, K.S., Nolta, J., Jia, J., Panganiban, B., Meng, L., Zhou, P., Shahnazari, M., et al. (2012). Directing mesenchymal stem cells to bone to augment bone formation and increase bone mass. Nat. Med. *18*, 456–462.

35. Debnath, S., Yallowitz, A.R., McCormick, J., Lalani, S., Zhang, T., Xu, R., Li, N., Liu, Y., Yang, Y.S., Eiseman, M., et al. (2018). Discovery of a periosteal stem cell mediating intramembranous bone formation. Nature *562*, 133–139.

36. Kotake, S., and Nanke, Y. (2014). Effect of TNFα on osteoblastogenesis from mesenchymal stem cells. Biochim. Biophys. Acta *1840*, 1209–1213.

37. Yang, S., Xie, C., Chen, Y., Wang, J., Chen, X., Lu, Z., June, R.R., and Zheng, S.G. (2019). Differential roles of TNFα-TNFR1 and TNFα-TNFR2 in the differentiation and function of $CD4^{+}Foxp3^{+}$ induced Treg cells in vitro and in vivo periphery in autoimmune diseases. Cell Death Dis. *10*, 27.

38. Yang, S., Wang, J., Brand, D.D., and Zheng, S.G. (2018). Role of TNF-TNF Receptor 2 Signal in Regulatory T Cells and Its Therapeutic Implications. Front. Immunol. *9*, 784.

39. Granero-Moltó, F., Weis, J.A., Miga, M.I., Landis, B., Myers, T.J., O'Rear, L., Longobardi, L., Jansen, E.D., Mortlock, D.P., and Spagnoli, A. (2009). Regenerative effects of transplanted mesenchymal stem cells in fracture healing. Stem Cells *27*, 1887–1898.

40. D' Alimonte, I., Nargi, E., Mastrangelo, F., Falco, G., Lanuti, P., Marchisio, M., Miscia, S., Robuffo, I., Capogreco, M., Buccella, S., et al. (2011). Vascular endothelial growth factor enhances in vitro proliferation and osteogenic differentiation of human dental pulp stem cells. J. Biol. Regul. Homeost. Agents *25*, 57–69.

41. Granstein, R.D. (2002). The skinny on CD39 in immunity and inflammation. Nat. Med. *8*, 336–338.

42. Linden, J., Koch-Nolte, F., and Dahl, G. (2019). Purine Release, Metabolism, and Signaling in the Inflammatory Response. Annu. Rev. Immunol. *37*, 325–347.

43. Antonioli, L., Pacher, P., Vizi, E.S., and Haskó, G. (2013). CD39 and CD73 in immunity and inflammation. Trends Mol. Med. *19*, 355–367.

44. Park, Y.J., Ryu, H., Choi, G., Kim, B.S., Hwang, E.S., Kim, H.S., and Chung, Y. (2019). IL-27 confers a protumorigenic activity of regulatory T cells via CD39. Proc. Natl. Acad. Sci. USA *116*, 3106–3111.

45. Schiavon, V., Duchez, S., Branchtein, M., How-Kit, A., Cassius, C., Daunay, A., Shen, Y., Dubanchet, S., Colisson, R., Vanneaux, V., et al. (2019). Microenvironment tailors nTreg structure and function. Proc. Natl. Acad. Sci. USA *116*, 6298–6307.

46. Gu, J., Ni, X., Pan, X., Lu, H., Lu, Y., Zhao, J., Guo Zheng, S., Hippen, K.L., Wang, X., and Lu, L. (2017). Human $CD39^{hi}$ regulatory T cells present stronger stability and function under inflammatory conditions. Cell. Mol. Immunol. *14*, 521–528.

47. Zhang, X., Ouyang, X., Xu, Z., Chen, J., Huang, Q., Liu, Y., Xu, T., Wang, J., Olsen, N., Xu, A., and Zheng, S.G. (2019). CD8+CD103+ iTregs Inhibit Chronic Graft-versus-

Host Disease with Lupus Nephritis by the Increased Expression of CD39. Mol. Ther. *27*, 1963–1973.

48. Liu, Z.M., Wang, K.P., Ma, J., and Guo Zheng, S. (2015). The role of all-trans retinoic acid in the biology of Foxp3+ regulatory T cells. Cell. Mol. Immunol. *12*, 553–557.
49. Li, Z., Lin, F., Zhuo, C., Deng, G., Chen, Z., Yin, S., Gao, Z., Piccioni, M., Tsun, A., Cai, S., et al. (2014). PIM1 kinase phosphorylates the human transcription factor FOXP3 at serine 422 to negatively regulate its activity under inflammation. J. Biol. Chem. *289*, 26872–26881.
50. Bozec, A., and Zaiss, M.M. (2017). T Regulatory Cells in Bone Remodelling. Curr. Osteoporos. Rep. *15*, 121–125.
51. Kong, N., Lan, Q., Su, W., Chen, M., Wang, J., Yang, Z., Park, R., Dagliyan, G., Conti, P.S., Brand, D., et al. (2012). Induced T regulatory cells suppress osteoclastogenesis and bone erosion in collagen-induced arthritis better than natural T regulatory cells. Ann. Rheum. Dis. *71*, 1567–1572.
52. Mediero, A., and Cronstein, B.N. (2013). Adenosine and bone metabolism. Trends Endocrinol. Metab. *24*, 290–300.
53. Carroll, S.H., Wigner, N.A., Kulkarni, N., Johnston-Cox, H., Gerstenfeld, L.C., and Ravid, K. (2012). A2B adenosine receptor promotes mesenchymal stem cell differentiation to osteoblasts and bone formation in vivo. J. Biol. Chem. *287*, 15718–15727.
54. Shih, Y.-R.V., Liu, M., Kwon, S.K., Iida, M., Gong, Y., Sangaj, N., and Varghese, S. (2019). Dysregulation of ectonucleotidase-mediated extracellular adenosine during postmenopausal bone loss. Sci. Adv. *5*, eaax1387.
55. Angers, S., and Moon, R.T. (2009). Proximal events in Wnt signal transduction. Nat. Rev. Mol. Cell Biol. *10*, 468–477.
56. Long, F. (2011). Building strong bones: molecular regulation of the osteoblast lineage. Nat. Rev. Mol. Cell Biol. *13*, 27–38.
57. Behrens, J., von Kries, J.P., Kühl, M., Bruhn, L., Wedlich, D., Grosschedl, R., and Birchmeier, W. (1996). Functional interaction of beta-catenin with the transcription factor LEF-1. Nature *382*, 638–642.
58. Liu, F., Kohlmeier, S., and Wang, C.Y. (2008). Wnt signaling and skeletal development. Cell. Signal. *20*, 999–1009.
59. Koide, M., Kobayashi, Y., Yamashita, T., Uehara, S., Nakamura, M., Hiraoka, B.Y., Ozaki, Y., Iimura, T., Yasuda, H., Takahashi, N., and Udagawa, N. (2017). Bone Formation Is Coupled to Resorption Via Suppression of Sclerostin Expression by Osteoclasts. J. Bone Miner. Res. *32*, 2074–2086.
60. Kramer, I., Halleux, C., Keller, H., Pegurri, M., Gooi, J.H., Weber, P.B., Feng, J.Q., Bonewald, L.F., and Kneissel, M. (2010). Osteocyte Wnt/beta-catenin signaling is required for normal bone homeostasis. Mol. Cell. Biol. *30*, 3071–3085.
61. Canalis, E. (2013). Wnt signalling in osteoporosis: mechanisms and novel therapeutic approaches. Nat. Rev. Endocrinol. *9*, 575–583.
62. Zhang, X., Zeng, D., Huang, F., and Wang, J. (2019). A protocol for isolation and culture of mesenchymal stem cells from human gingival tissue. Am. J. Clin. Exp. Immunol. *8*, 21–26.
63. Lefèvre, S., Knedla, A., Tennie, C., Kampmann, A., Wunrau, C., Dinser, R., Korb, A., Schnäker, E.M., Tarner, I.H., Robbins, P.D., et al. (2009). Synovial fibroblasts spread rheumatoid arthritis to unaffected joints. Nat. Med. *15*, 1414–1420.
64. Gulati, G.S., Murphy, M.P., Marecic, O., Lopez, M., Brewer, R.E., Koepke, L.S., Manjunath, A., Ransom, R.C., Salhotra, A., Weissman, I.L., et al. (2018). Isolation and functional assessment of mouse skeletal stem cell lineage. Nat. Protoc. *13*, 1294–1309.